

Rainfall Extremes In Northern And Southern Central Java Coasts: Comparative Study Of ENSO And IOD Influences

Imawan Mashuri¹, Muhammad Labieb Muzakkie^{1*}, Duo Rahman Abdilah¹, Salsabila Nurul Izzah¹, Dan Giarno¹

¹Program Studi Klimatologi, Sekolah Tinggi Meteorologi Klimatologi dan Geofisika, Kota Tangerang, Banten, Indonesia

***E-mail:** muhammad.labieb.muzakkie.24@gmail.com

Received: 06 01 2025 / Accepted: 30 06 2025 / Published online: 24 07 2025

ABSTRAK

Wilayah pesisir Utara dan Selatan Jawa Tengah kerap mengalami bencana hidrometeorologi akibat curah hujan ekstrem. Keterkaitan antara curah hujan ekstrem di kedua wilayah ini dipengaruhi oleh fluktuasi IOD dan ENSO. Tujuan penelitian yaitu membandingkan karakteristik curah hujan ekstrem di wilayah pesisir utara dan selatan Jawa Tengah dengan kaitannya terhadap ENSO dan IOD. Metode analisis curah hujan ekstrem menggunakan Indeks curah hujan ekstrem (RX1D, RX5D, CDD, CWD) dan korelasi Spearman-rank guna memahami pengaruh fenomena dan indeks. Hasil menunjukkan bahwa RX1D dan RX5D lebih tinggi selama La Niña dan IOD negatif, terutama di musim hujan, sementara El Niño dan IOD positif menurunkan nilainya. CWD lebih panjang saat La Niña, namun IOD positif mengurangi jumlah hari hujan, khususnya pada musim kemarau. Sebaliknya, CDD meningkat signifikan selama El Niño dan IOD positif yang memperkuat hari kering, khususnya di pesisir selatan. Korelasi Spearman-Rank menunjukkan korelasi negatif ENSO dan IOD terhadap RX1D, RX5D, dan CWD, serta hubungan positif terhadap CDD, dengan pengaruh lebih kuat di musim kemarau dan peralihan kedua (SON) serta variasi karakteristik di kedua wilayah pesisir. Temuan ini menunjukkan perlunya strategi adaptasi dan mitigasi terhadap karakteristik hujan ekstrem ketika Fase ENSO dan IOD terjadi secara bersamaan dengan pengaruh lebih kuat di pesisir selatan.

Kata Kunci: Hujan Ekstrem, ENSO, IOD, Pesisir

ABSTRACT

The northern and southern coastal regions of Central Java frequently experience hydrometeorological disasters due to extreme rainfall. The relationship between extreme rainfall in these two areas is influenced by fluctuations in the Indian Ocean Dipole (IOD) and the El Niño-Southern Oscillation (ENSO). This study aims to compare the characteristics of extreme rainfall in the northern and southern coastal regions of Central Java in relation to ENSO and IOD phases. The analysis applies extreme rainfall indices (RX1D, RX5D, CDD, CWD) and Spearman-rank correlation to understand the influence of these climate phenomena and indices. The results show that RX1D and RX5D values are higher during La Niña and negative IOD phases, especially in the rainy season, while El Niño and positive IOD phases reduce their intensity. CWD is longer during La Niña, but positive IOD decreases the number of rainy days, particularly during the dry season. In contrast, CDD increases significantly during El Niño and positive IOD, which intensify dry conditions, especially along the southern coast. Spearman-rank correlations indicate a negative relationship between ENSO/IOD and RX1D, RX5D, and CWD, and a positive relationship with CDD, with stronger impacts during the dry season and second transitional period (SON), as well as varying characteristics between the two coasts. These findings underscore the necessity for adaptation and mitigation strategies in response to extreme rainfall characteristics, particularly when ENSO and IOD phases coincide, with stronger impacts observed along the southern coast.

Keywords: Extreme Rainfall, ENSO, IOD, Coastal

INTRODUCTION

Global climate change has significantly impacted weather and climatic patterns across various regions and countries. In 2023, the Intergovernmental Panel on Climate Change (IPCC) reported that intense rainfall and flooding are expected to increase in frequency and intensity across much of Africa and Asia (Lee et al., 2023). Additionally, climate change has caused uneven rainfall distribution (Nandargi & Barman, 2018). In Indonesia, one clear manifestation of climate change is the alteration in rainfall patterns and extreme temperatures, which have profound implications for ecosystems and community activities (Rahayu et al., 2020). Climate change affects not only agricultural and fisheries sectors (Ikhwal et al., 2022; Rahman et al., 2021), but also escalates the frequency of hydrometeorological disasters such as floods, landslides, and droughts (Agustina et al., 2020; Darmawan et al., 2023; Veanti & Kloster, 2018).

The coastal regions of Central Java are among the areas most frequently affected by flooding, occurring in both the northern and southern coasts due to extreme rainfall (Amri & Giarno, 2024; Giarno & Nanaruslana, 2022). However, these two coastal regions exhibit significantly different geographical and climatic characteristics. The northern coast of Central Java borders the relatively shallow and calm Java Sea (Nabila et al., 2019), while the southern coast faces the deep and high-wave Indian Ocean (Setyawan & Pamungkas, 2017). Previous studies indicate that the northern coast receives higher rainfall than the southern coast (Raharja et al., 2022). The southern coast is more sensitive to sea surface temperature variations in the Indian Ocean, which intensify extreme weather dynamics during the dry season and

increase drought risks (Mardiansyah et al., 2018).

Research by Fadlan et al. (2017) and Kunarso et al. (2011), highlighted the atmospheric-oceanic dynamics of the northern and southern coasts of Java, influenced by several atmospheric phenomena, such as the monsoon, ENSO (El Niño-Southern Oscillation), and IOD (Indian Ocean Dipole). These phenomena directly contribute to the frequency of tidal floods, droughts, and changes in sea level. ENSO, a climate anomaly in the Pacific Ocean characterized by increased sea surface temperatures, and IOD, driven by sea surface temperature anomalies in the western and eastern Indian Ocean, both influence rainfall patterns in Java (Rahayu et al., 2018).

The link between extreme rainfall in these two coastal regions is shaped by fluctuations in IOD and ENSO, which increase the frequency and intensity of rainfall during certain seasons. During El Niño events coinciding with positive IOD, significant reductions in seasonal rainfall averages occur during the SON (September–November) and DJF (December–February) periods in Central Java (Abdullah, 2021). Conversely, during La Niña events and negative IOD, average rainfall in Central Java increases during DJF-MAM (March–May), with extreme rainfall events occurring more frequently (Yunus, 2015). Compared to the northern coast, the southern coast of Java demonstrates greater sensitivity to IOD conditions, where negative IOD can increase sea surface temperatures and exacerbate extreme rainfall (Yulihastin et al., 2021). Meanwhile, on the northern coast, La Niña or negative IOD also results in increased rainfall during the wet season, though the intensity of extreme rainfall is generally lower than that of the southern coast. Research by Kurniadi et al. (2021) revealed that rainfall in the northern region tends to be more stable throughout the

year, with monsoon cycles playing a more significant role than Indian Ocean sea surface temperature changes, which predominantly affect the southern coast.

Most prior studies on extreme rainfall and temperature have been limited to specific coastal regions such as Serang and Jakarta, without exploring inter-regional comparisons or ocean-atmosphere linkages (Hidayat et al., 2018; Suwarman et al., 2022). Other studies have primarily compared the climatic characteristics of mountainous and coastal areas, highlighting spatial variability in rainfall driven by topography and monsoonal influences, without specifically focus on rainfall extremes (Afghani et al., 2023; Aldrian & Djamil, 2008; Anam et al., 2023). Therefore, the study aims to compare the characteristics of extreme rainfall in the northern and southern coastal regions of Central Java. This analysis is expected to provide a robust scientific basis for climate change mitigation and adaptation efforts, particularly in addressing the impacts of climatic phenomena on hydrometeorological disasters in the vulnerable coastal areas of Central Java Province.

RESEARCH METHODS

Research Period and Location

This study was conducted in Central Java Province, Indonesia, with a particular focus on comparing the northern and southern coastal regions. These two coastal areas exhibit distinct geographical characteristics. The northern coast, which faces the Java Sea, is generally flatter and more urbanized, with lower elevation. In contrast, the southern coast, which borders the Indian Ocean, is characterized by more rugged terrain and higher elevation.

To capture the differences, rainfall data were collected from six rain posts managed by the Meteorological, Climatological, and Geophysical Agency

(BMKG). The northern coast is represented by the Klampok, Weleri, and Rembang Pelabuhan rain posts, while the southern coast is represented by the Rantewringin, Ngombol, and Pracimantoro rain posts. These rain posts were selected based on the completeness and quality of their daily rainfall data, ensuring reliable analysis of extreme rainfall characteristics in both northern and southern coastal regions of Central Java. The geographical locations of these rain posts are detailed in Figure 1.

Research Data

The data utilized in this study include daily rainfall observations collected from six rain posts over 24 years (2000–2023). For the identification of the El Niño Southern Oscillation (ENSO) phases, data were obtained from the National Oceanic and Atmospheric Administration (NOAA) and downloaded from

https://origin.cpc.ncep.noaa.gov/products/analysis_monitoring/ensostuff/detrend.Niño34.ascii.txt. Similarly, for the identification of Indian Ocean Dipole (IOD) phases, data were sourced from NOAA and downloaded from https://www.cpc.ncep.noaa.gov/products/international/ocean_monitoring/indian/IODMI/DMI_month.html.

Method

The annual average patterns of extreme climate indices from 2000–2023, as well as during years of El Niño, La Niña, negative IOD, and positive IOD events, were plotted to observe variations in extreme rainfall indices for each of these occurrences. The plots were generated for three rain posts located in the northern coastal region of Central Java and three rain posts in the southern coastal region of Central Java. By plotting extreme rainfall data for each phase of ENSO and IOD, it is possible to analyze how these phases

influence extreme rainfall monthly. These plots also enable a comparative analysis of extreme climate conditions between the northern and southern coastal regions of

Central Java, as well as the differing impacts of ENSO and IOD on extreme climate events in these two areas.

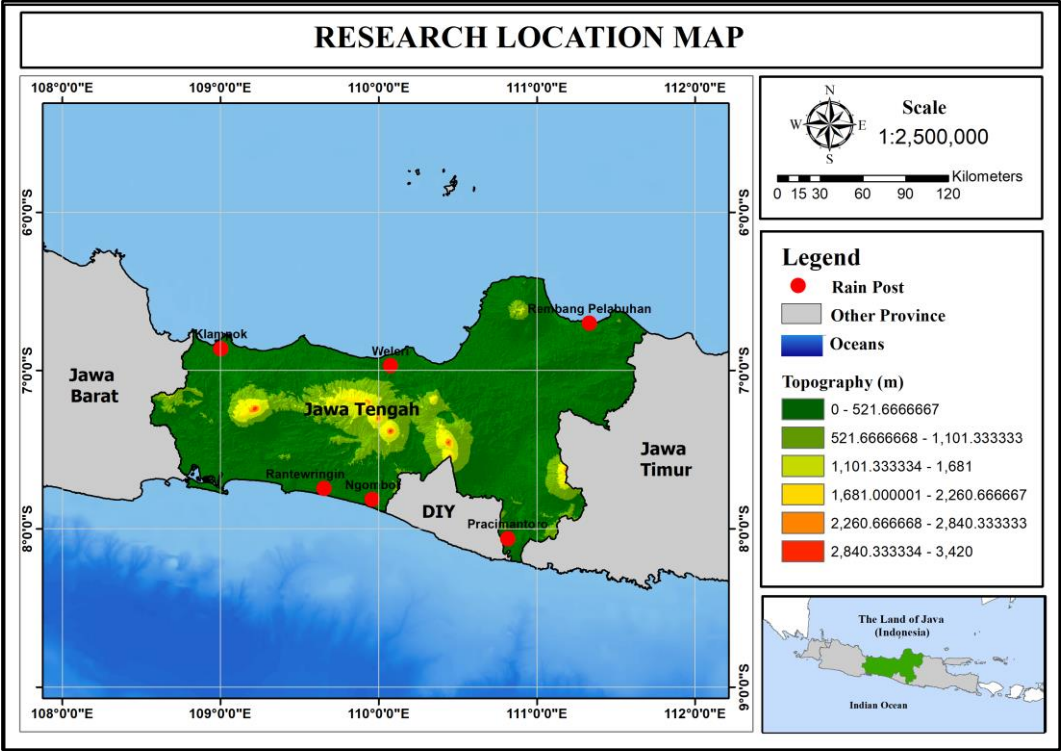


Figure 1. Research Location Map

The historical identification of ENSO event years was conducted by examining 5-period running averages (NOAA, 2025), while the identification of IOD event years

was performed by analyzing 3-month running averages (JMA, 2002). A detailed summary of these identifications is presented in Table 1.

Table 1. ENSO & IOD Years and Their Combinations

	El Niño	Normal	La Niña
Positive IOD	2015, 2019, 2023	2012	-
Normal	2002, 2004, 2009	2001, 2003, 2006, 2013, 2014, 2017, 2018	2000, 2007, 2008, 2011, 2010, 2020, 2021
Negative IOD	2016	2005, 2014	2022

Source: NOAA & JMA

The study utilized extreme rainfall indices developed by the CCI/CLIVAR/JCOMM team under the ETCCDI (Expert Team on Climate

Change Detection and Indices) project to analyze extreme rainfall. A total of 27 climate indices have been developed by ETCCDI based on temperature and rainfall

(Donat et al., 2013). The indices measured in this research include the highest one-day rainfall (RX1D), the total highest rainfall over five consecutive days (RX5D), the number of consecutive dry days (CDD), and the number of consecutive wet days

(CWD). The calculation of extreme rainfall indices in this study was performed using Python. A detailed description of the indices used in this research is provided in Table 2.

Table 2. Climate Extreme Indices

Index	Description	Unit	Formula
RX1D	Highest daily rainfall	mm	$R1XD = \max (RR_d)$ RR: daily rainfall d: day
RX5D	Total highest rainfall in 5 consecutive days	mm	$R5XD = \max (RR_f)$ R: daily rainfall f: 5-day interval
CWD	Consecutive wet days	day	<i>Consecutive</i> ($RR_d \geq 1$ mm) RR: daily rainfall d: day
CDD	Consecutive dry days	day	<i>Consecutive</i> ($RR_d < 1$ mm) RR: daily rainfall d: day

The monthly ENSO index (Niño 3.4) and Indian Ocean Dipole (IOD) index, derived from NOAA data, were utilized in a correlation analysis to investigate the relationship between extreme rainfall indices and the ENSO and IOD phenomena. The objective of the correlation analysis was to determine how ENSO and/or IOD influence extreme rainfall events along the southern and northern coastal regions of Central Java.

The Spearman-rank partial correlation technique was employed to analyze the relationships among three variables: extreme rainfall indices, the Indian Ocean Dipole (IOD), and Niño 3.4. Spearman's rank correlation coefficient is a non-parametric statistical measure used to evaluate the strength and direction of

monotonic relationships between two ranked variables or between a ranked variable and a measured variable (Xiao et al., 2016). The equation for calculating Spearman's rank partial correlation is given in Equation 1 (Zar, 2005):

$$r_s = 1 - \frac{6 \sum d_i^2}{N(N-1)^2} \tag{1}$$

where $d_i^2 = X'_i - Y'_i$ represents the squared difference between each pair of ranked variables and N denotes the total sample size. Equation 1 quantifies how closely the rankings of two variables correspond, with a smaller sum of squared differences indicating a stronger monotonic relationship. This correlation method was applied to independently

analyze the influence of ENSO and IOD on each extreme rainfall index based on the implemented methodology (Ashok & Saji,

2007; Hidayat et al., 2016). For further details, the research flowchart is presented in Figure 2.

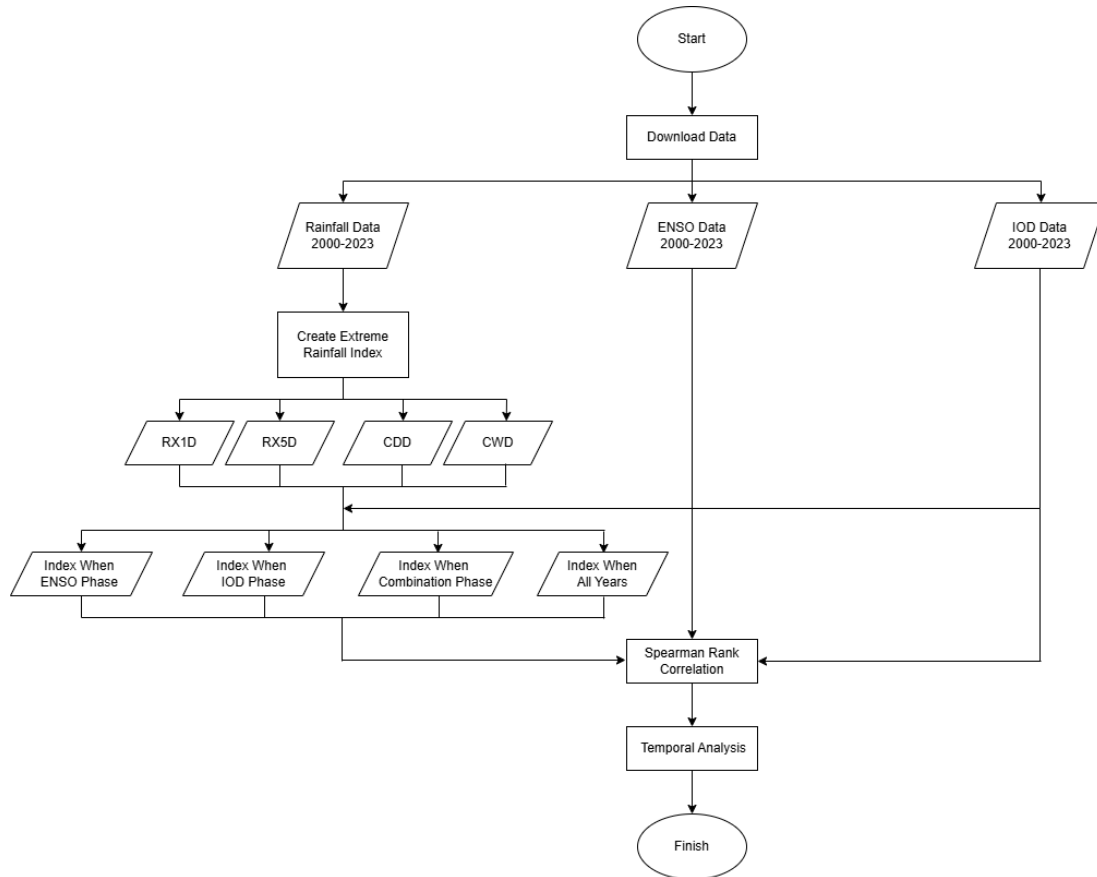


Figure 2. Research Flowchart

Results and Discussion

RX1D Index

Figure 3 illustrates the RX1D values at six rain posts across the northern and southern coasts of Central Java. During the rainy season (DJF), all rain posts exhibit an increase in monthly mean RX1D across all years, whereas the lowest values occur during the dry season (JJA). This pattern is influenced by the alternating dominance of the Asian and Australian monsoon winds, affecting rainfall intensity in both regions. Notably, the southern coast records consistently higher RX1D averages compared to the

northern coast, suggesting stronger local rainfall dynamics.

During La Niña phases, RX1D values at all rain posts are generally higher than the all-year mean, except for certain months at Ngombol, Klampok, Rantewaringin, and Weleri rain posts. Conversely, El Niño phases correspond to lower RX1D values. The anomaly is more pronounced along the southern coast, indicating that ENSO has a stronger and more significant impact on extreme rainfall in this region compared to the northern coast, albeit with variability among rain posts. This finding aligns with studies on ENSO's regional

hydrometeorological influence (Hidayat et al., 2016).

The influence of IOD phases on RX1D is less uniform. During negative IOD phases, RX1D anomalies are particularly significant during the dry season (JJA), where most rain posts exhibit higher than average values. These anomalies often surpass those observed during La Niña phases, suggesting that negative IOD has a stronger influence on RX1D during JJA. In contrast, positive IOD phases generally result in lower RX1D values, with exceptions in certain months at Pracimantoro, Rantewaringin, and Weleri rain posts. The variability of RX1D during IOD phases underscores the complexity of its impact compared to

ENSO, as supported by previous research (Ashok & Saji, 2007).

The enhanced extreme rainfall during this phase highlights the reinforcing interaction between La Niña and negative IOD. This combination results in the highest RX1D anomalies across all rain posts, particularly along the southern coast, except during January and February. When El Niño and Positive IOD combination phase, RX1D values are typically lower than the all-year mean at northern rain posts and to a lesser extent at southern rain posts, with occasional positive anomalies. This phase demonstrates a synergistic effect, where positive IOD amplifies El Niño's suppressive impact on extreme rainfall.

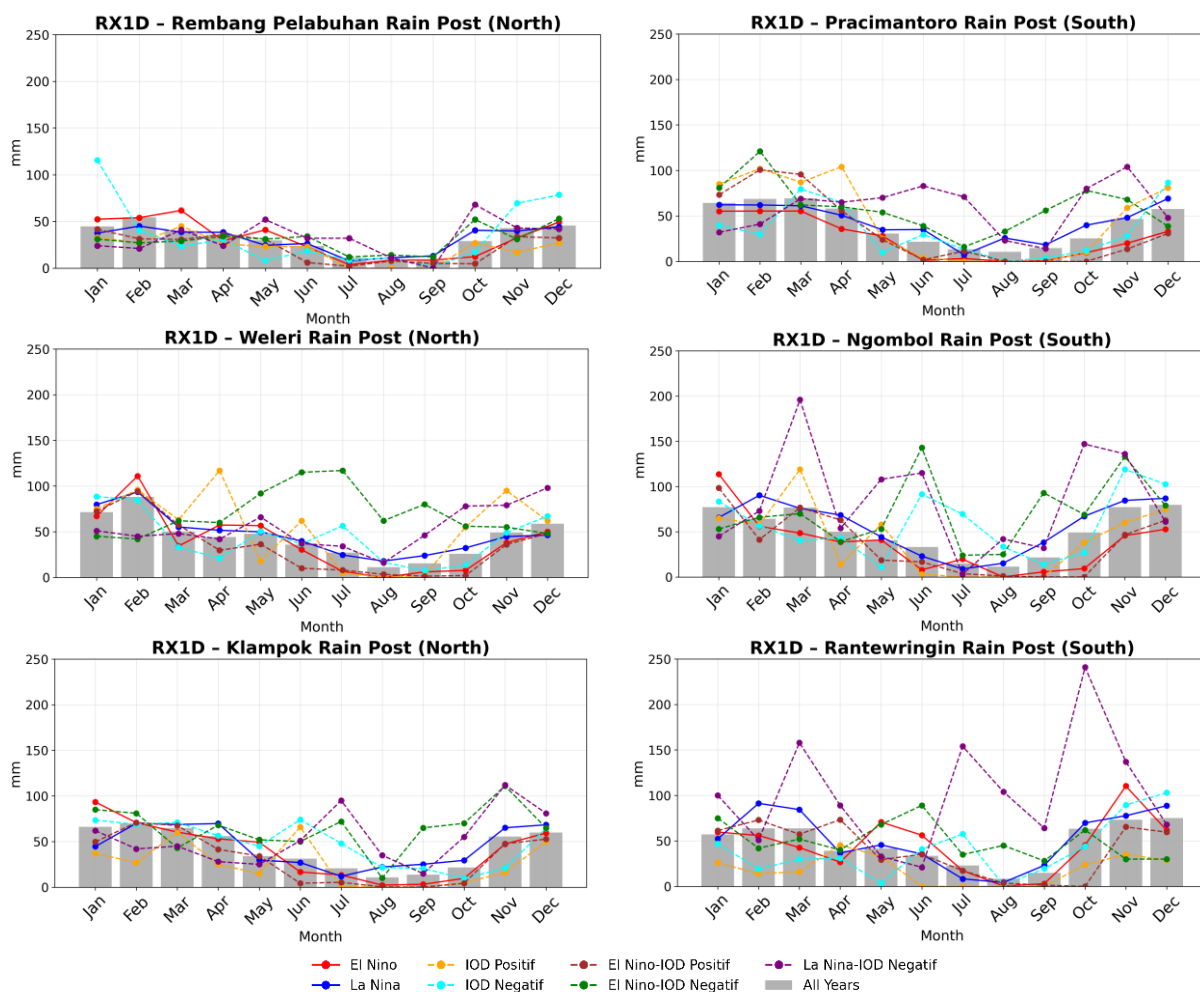


Figure 3. RX1D Index Values at Each Rain Post Along The Northern Coast of Central Java (Left) and The Southern Coast of Central Java (Right).

RX5D Index

Figure 4 illustrates the monthly mean RX5D values across the northern and southern coasts of Central Java. During all-year periods, RX5D increases during the dry seasons (JJA, SON) and decreases during wet seasons (DJF, MAM). This pattern reflects the dominant influence of Asian and Australian monsoons on rainfall variability. Despite similar seasonal trends, RX5D values along the southern coast are consistently higher than those along the northern coast, suggesting stronger extreme rainfall dynamics in the south.

RX5D is generally higher during La Niña and lower during El Niño compared to the all-year mean, highlighting the significant influence of ENSO on extreme rainfall. Notably, anomalies are more pronounced in the southern coast, where ENSO exerts a stronger effect. However, some months deviate from this general trend, reflecting localized variability. These findings align with prior studies on ENSO's role in modulating extreme rainfall (Hidayat et al., 2016).

Negative IOD phases show varying impacts on RX5D across rain posts. In rain posts such as Weleri, Klampok, Ngombol, and Rantewaringin, RX5D increases significantly during the dry season (JJA), often surpassing values observed during La Niña. This suggests a notable role of negative IOD in enhancing extreme rainfall during dry periods. Conversely, during positive IOD phases, RX5D is generally lower than the all-year mean, except for anomalies observed at Weleri rain post. These results indicate that El Niño typically has a stronger influence on RX5D than positive IOD, although the impacts are more pronounced along the southern coast.

The enhancement of extreme rainfall is most pronounced during the phase, underscoring the synergistic effect of La Niña and negative IOD in amplifying rainfall intensity. This combination results in the highest RX5D values across all rain posts, particularly along the southern coast. When El Niño and Positive IOD combination phase, RX5D decreases across all northern rain posts and most southern rain posts, with occasional positive anomalies in specific months. The combined effect of these phases suppresses extreme rainfall more significantly than either phase alone.

CWD Index

Figure 5 highlights the seasonal variability of the CWD index across the northern and southern coasts of Central Java. During the wet season (DJF), CWD values increase, indicating longer consecutive wet days, whereas in the dry season (JJA), CWD values decline. The southern coast consistently shows higher CWD values compared to the northern coast, reflecting prolonged rainfall durations likely due to enhanced moisture transport from the Indian Ocean via the Asian monsoon. This supports the southern coast's role as a primary rainfall recipient (McBride & Nicholls, 1983).

During La Niña, CWD increases across all rain posts, with more pronounced effects along the southern coast, except for isolated deviations in some months (e.g., Pracimantoro, Klampok). Conversely, during El Niño, CWD generally decreases, particularly in the southern region, underscoring ENSO's stronger impact on rainfall continuity in this area. The results align with findings that La Niña enhances moisture convergence, while El Niño suppresses it (Supari et al., 2018).

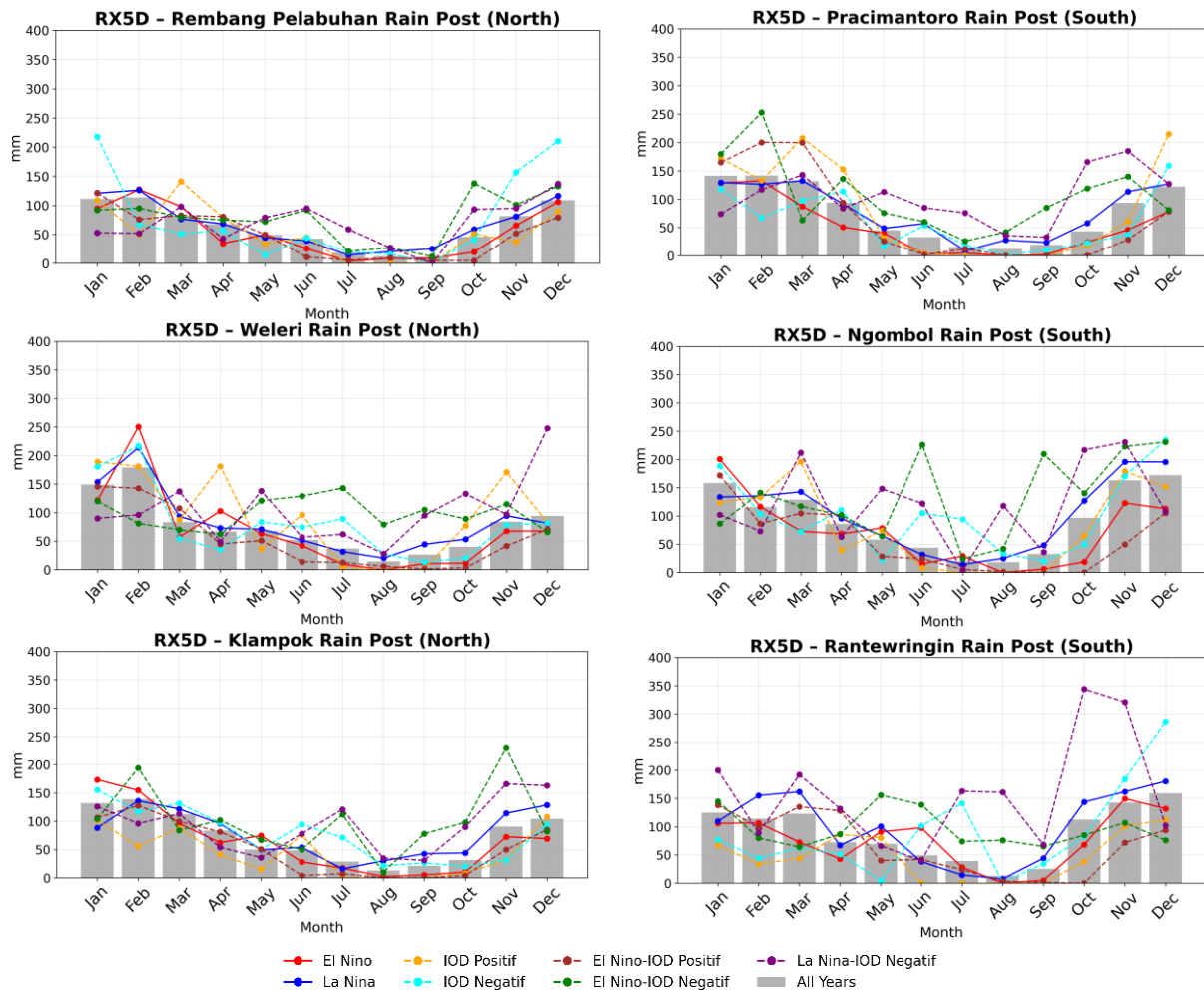


Figure 4. RX5D Index Values at Each Rain Post Along The Northern Coast of Central Java (Left) and The Southern Coast of Central Java (Right).

Negative IOD phases show varied effects, with slight CWD increases during dry months (JJA) due to light rainfall events. However, CWD values remain lower than during La Niña, given the less continuous rainfall associated with negative IOD. Positive IOD phases reduce CWD significantly in both regions, although anomalies of increased wet days occur in wet months at specific rain posts (e.g., Weleri, Rantewaringin). Overall, IOD impacts on CWD are more variable than ENSO, highlighting the complexity of IOD-driven rainfall dynamics (Cai et al., 2014).

The combination of La Niña and Negative IOD produces the highest CWD values, particularly along the southern coast, indicating the synergistic enhancement of rainfall duration. Anomalies are positive across most months, though some exceptions occur (e.g., January). This phase underscores the amplifying effect of simultaneous La Niña and negative IOD on extreme rainfall continuity. In contrast, El Niño and Positive IOD combined effects result in significantly shorter CWD across both regions, emphasizing drier conditions compared to either phase occurring alone.

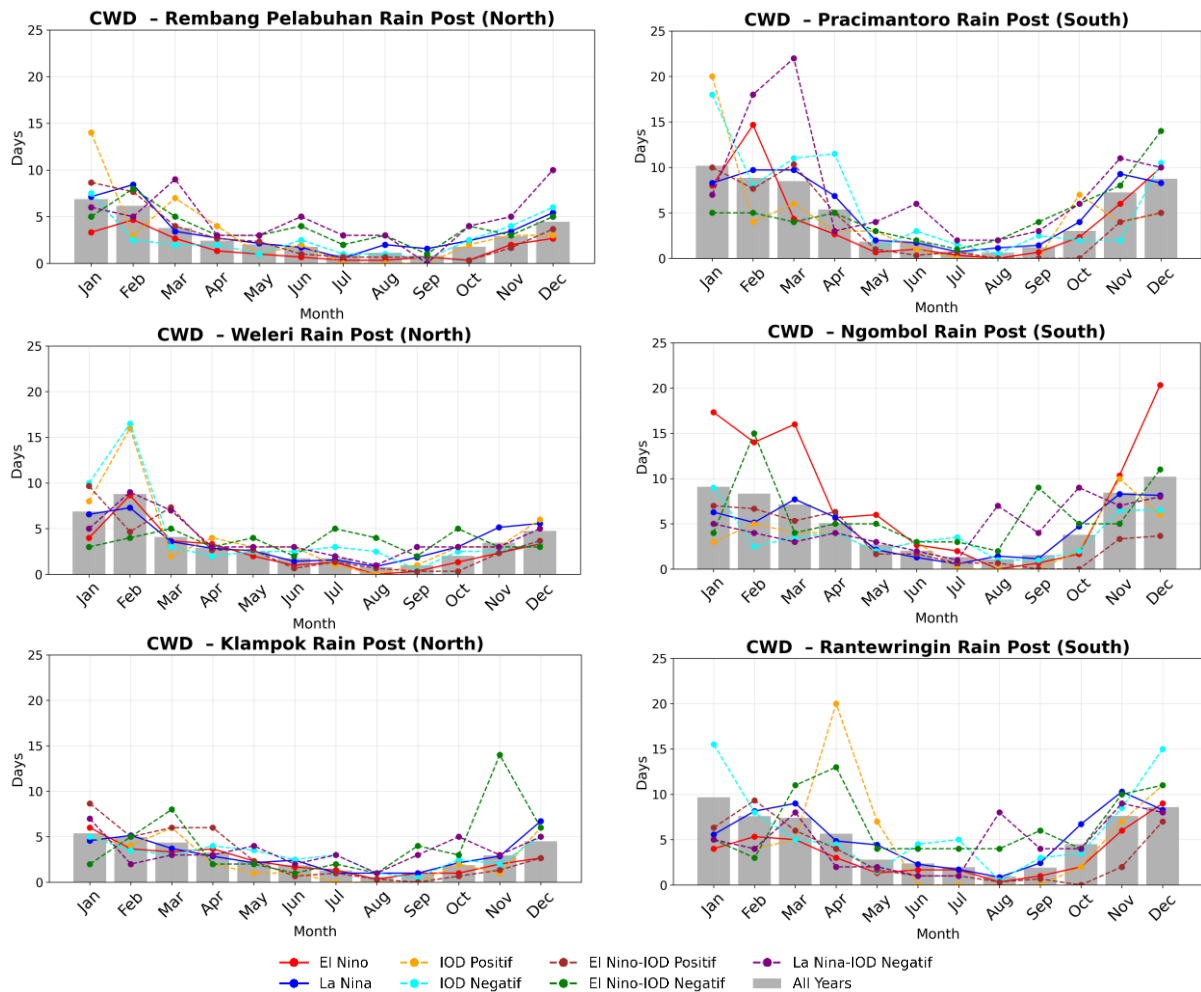


Figure 5. CWD Index Values at Each Rain Post Along The Northern Coast of Central Java (Left) and The Southern Coast of Central Java (Right)

CDD Index

Figure 6 highlights the seasonal variability of the CDD index across northern and southern coasts of Central Java. In the northern region, CDD durations are generally shorter than in the southern region, particularly during the transitional months of September and October. During El Niño years, a substantial increase in CDD is observed, with locations such as Rembang Pelabuhan and Weleri recording durations exceeding 60 days. Conversely, La Niña conditions result in shorter CDD durations, approaching the monthly climatological averages. Positive Indian Ocean Dipole (IOD) events exhibit a similar impact to El

Niño, with notable increases in CDD at rain posts like Rembang Pelabuhan and Klampok, albeit with slightly lower impacts at Weleri. Meanwhile, negative IOD events significantly suppress CDD durations, particularly during the dry season.

In the southern coastal region, CDD durations are consistently longer than in the north, peaking in September. Strong El Niño events exacerbate CDD durations at rain posts like Pracimantoro, though their influence is negligible at Ngombol and Rantewringin. The combined effects of El Niño and positive IOD exacerbate drought conditions, with

Pracimantoro and Ngombol recording extreme CDD durations exceeding 140 days. In contrast, La Niña and negative IOD events markedly reduce CDD durations, aligning them closer to monthly averages. This reduction is particularly significant during the peak dry season (June to August).

The combined influence of El Niño and positive IOD in the southern region amplifies CDD durations compared to the

northern region, emphasizing the southern coast's higher vulnerability to prolonged dry spells. This analysis underscores that the southern coastal region is more significantly impacted by ENSO and IOD phenomena, leading to pronounced changes in CDD patterns, both in terms of increases during dry conditions and reductions during wetter periods (Supari et al., 2018).

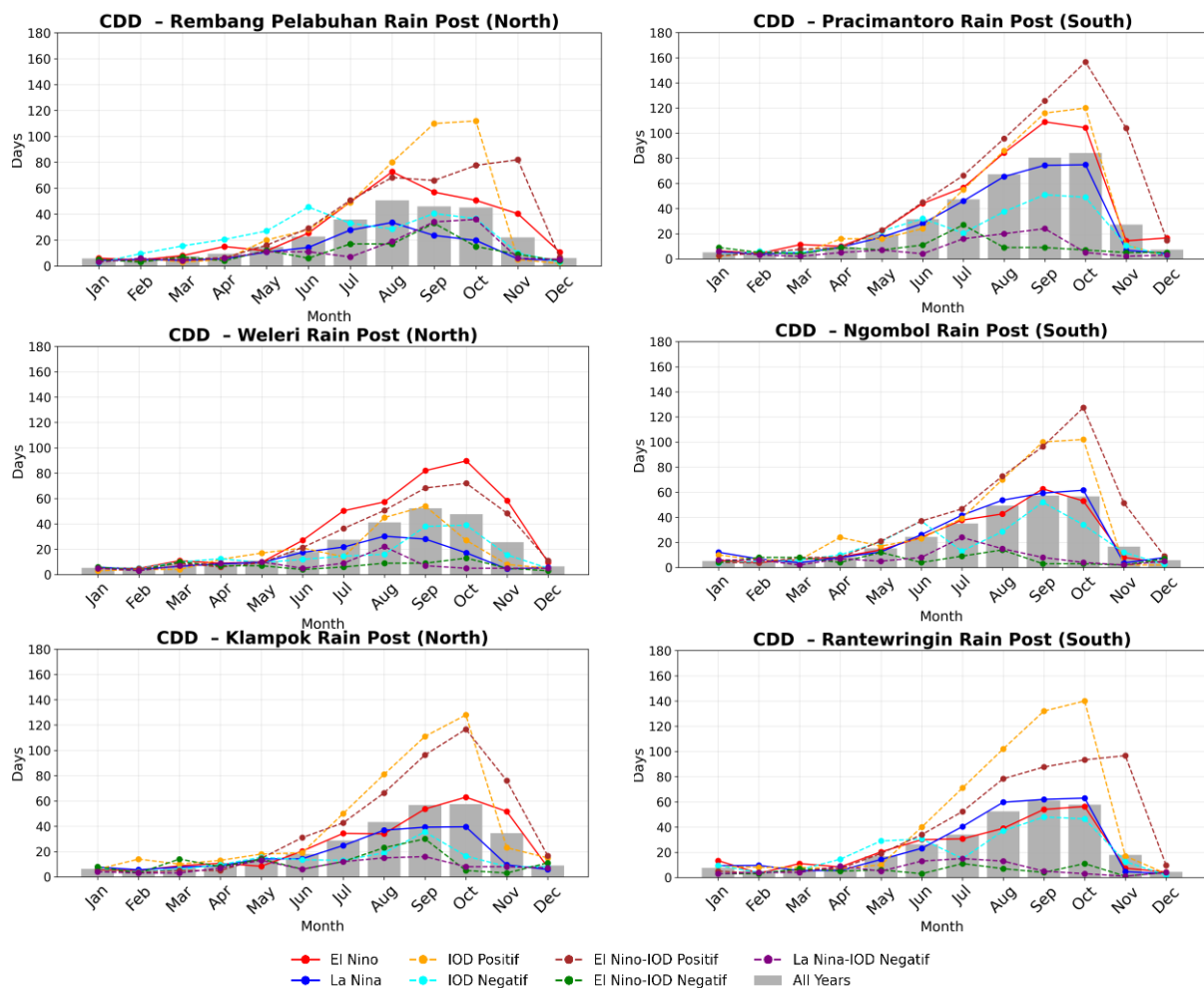


Figure 6. CDD Index Values at Each Rain Post Along The Northern Coast of Central Java (Left) and The Southern Coast of Central Java (Right)

Correlation of ENSO to Extreme Rainfall Indices

The Spearman rank correlation between ENSO and the RX1D index in

northern and southern coastal regions of Central Java is predominantly negative, indicating that El Niño tends to suppress extreme rainfall, while La Niña enhances

it. Strong negative correlations are observed in October across all locations, ranging from -0.50 to -0.70, particularly significant in southern coastal rain posts such as Weleri and Klampok. Similar patterns occur in August and September, albeit with slightly weaker intensities. Conversely, from January to May, correlations weaken and become inconsistent, reflecting the diminished influence of ENSO compared to local factors such as the Asian monsoon (McBride, 1998).

The correlation between ENSO and RX5D exhibits a similar pattern, with predominantly negative values, especially from July to November. Significant peaks in negative correlations occur in October, with values ranging from -0.61 to -0.78 across all locations. Strong correlations are also evident in August, such as at Weleri (-0.54) and Klampok (-0.41). However, during December to June, correlations weaken, indicating the dominance of the Asian monsoon in modulating extreme rainfall over ENSO effects (Trenberth, 1997). The variation in correlation intensity between northern and southern coasts suggests that local atmospheric dynamics play a crucial role in rainfall distribution.

The correlation between ENSO and the CWD index shows stronger influence during the dry season (July–October). The highest negative correlations are observed in October, such as at Rembang Pelabuhan (-0.70) and Weleri (-0.68), indicating that El Niño reduces wet days by increasing atmospheric pressure in the tropics (Hendon, 2003). At the beginning of the year (January–March), correlations are generally weaker or near zero, reflecting the dominant influence of the Asian monsoon. Toward the year's end, negative correlations strengthen again, highlighting El Niño's role in extending the dry season.

The correlation between ENSO and the CDD index reveals a significant positive relationship during the dry season (June–September), with peak values in August, such as at Rembang Pelabuhan (0.67) and Weleri (0.71). This indicates that El Niño prolongs dry spells by reducing atmospheric moisture (Goddard & Gershunov, 2020). Similar correlations are observed in southern coastal areas, though slightly weaker, such as at Pracimantoro (0.54 in August). Early in the year, correlations are low or negative, reflecting the rainy season's dominance, which diminishes ENSO's impact. These correlation patterns underscore ENSO's significant influence on dry-day durations in tropical regions (Figure 7).

Correlation of IOD to Extreme Rainfall Indices

The Spearman-Rank correlation between the Indian Ocean Dipole (IOD) and the RX1D index reveals a predominantly negative pattern across all locations, particularly during the dry season (June–October) (Figure 8). Significant negative correlations were identified along the southern coast of Central Java, with lower values than the northern coast, suggesting a stronger IOD influence in the south. For instance, in southern coastal areas like Ngombol, this influence reflects the role of a positive IOD in reducing extreme rainfall by increasing atmospheric pressure and decreasing humidity (Kurniadi et al., 2021). Weaker correlations during other months, such as January–May, reflect the dominance of monsoons and local factors that mitigate IOD's effect on RX1D (Biswas, 2023).

The relationship between IOD and RX5D also shows a predominantly negative pattern, particularly during the dry season (July–October). Strong to very strong correlations were identified in July and October across the region, for example, in Klampok and Weleri. This

pattern confirms that positive IOD tends to reduce extreme rainfall over five-day periods by affecting moisture distribution in the tropics (Alavinia & Zarei, 2021). Conversely, weak positive correlations were observed during February–April at

some locations, indicating an insignificant IOD influence during the first transition period, likely due to high humidity dominated by the monsoon (McBride, 1998).

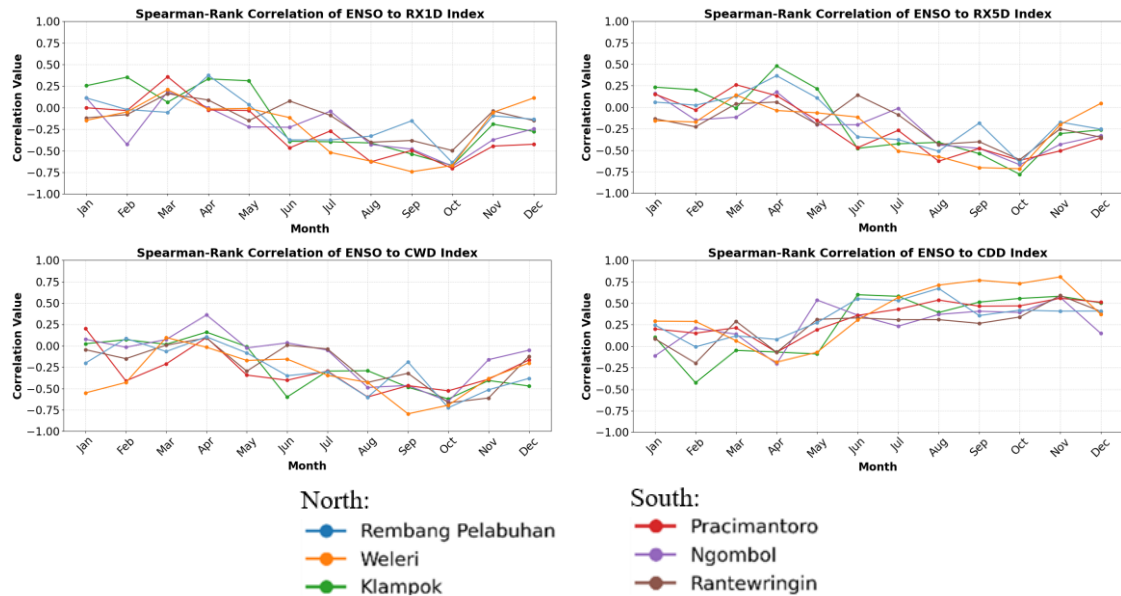


Figure 7. Correlation of ENSO to Extreme Rainfall Indices

CWD index shows a significant negative correlation with IOD during the dry season (July–October), particularly in locations like Klampok (-0.77) and Ngombol (-0.77) in October. This pattern indicates a reduction in wet days due to positive IOD, which increases atmospheric pressure over the eastern Indian Ocean (Saji et al., 1999). However, early in the year (January–March), the correlations tend to be weak or slightly positive, reflecting a neutral or negative IOD phase that supports rainfall along the coast (Ashok et al., 2001). This phenomenon underscores the dominant influence of IOD during the dry season compared to the wet season.

The Spearman-Rank correlation between IOD and CDD shows a strong

positive relationship during the dry season, particularly in August and September, with the highest values in Weleri (0.77) and Ngombol (0.77). This correlation indicates an increase in dry days during positive IOD phases due to reduced humidity and weakened monsoon winds (Chakraborty & Singhai, 2021). Early in the year (January–March), correlations tend to be low or negative, as seen in Ngombol (-0.51 in February), reflecting the dominance of the Asian monsoon, which reduces the IOD effect. Towards the end of the year (November–December), positive correlations reemerge, indicating a delayed transition from the dry season to the rainy season due to positive IOD.

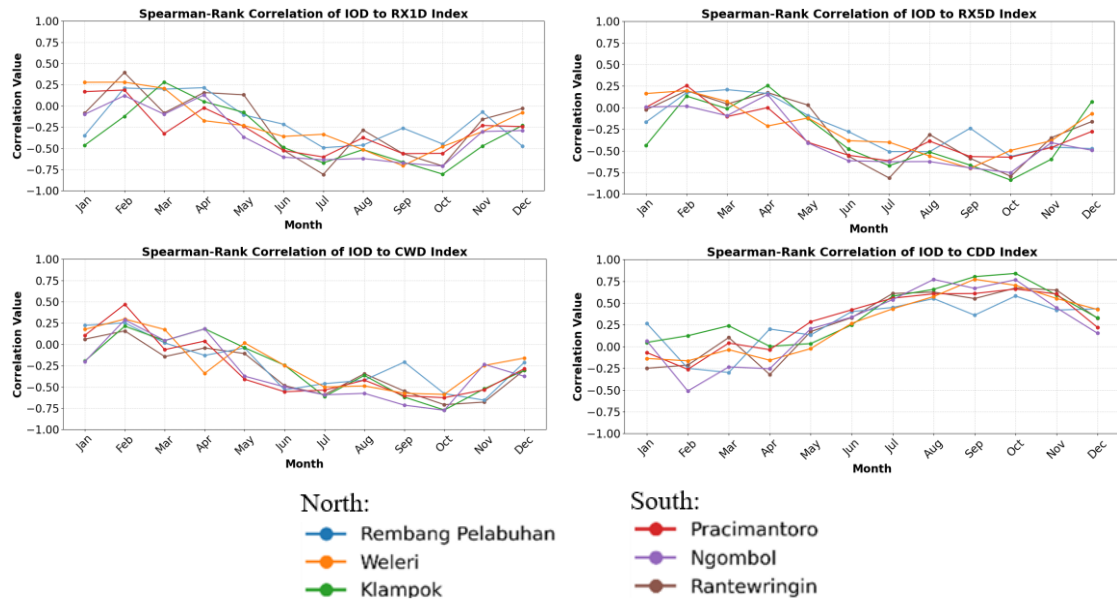


Figure 8. Correlation of IOD to Extreme Rainfall Indices

Conclusion

Extreme rainfall and the duration of rainy days and dry days in the northern and southern coastal regions of Central Java are influenced by ENSO (El Niño and La Niña) and the Indian Ocean Dipole (IOD). Under normal conditions, RX1D and RX5D are generally higher during the rainy season and lower during the dry season, with more intense extreme rainfall observed along the southern coast. La Niña and negative IOD increase extreme rainfall and extend the duration of continuous wet days (CWD), while El Niño and positive IOD intensify droughts, as indicated by longer durations of continuous dry days (CDD), particularly in the southern coastal areas.

The combination of ENSO and IOD has a greater impact compared to each phenomenon individually, with La Niña-negative IOD resulting in peak extreme rainfall and El Niño-positive IOD exacerbating drought conditions. The influence of ENSO on RX1D and RX5D is generally negative, especially during the dry season (June–September) and the second transitional season (October–November). Similarly, IOD typically

shows a negative correlation with RX1D and RX5D, particularly from July to October, with a stronger effect observed in the southern coastal areas. For the CWD index, both ENSO and IOD show a significant negative correlation during the dry season. Conversely, the CDD index exhibits a significant positive correlation, particularly during the dry season.

The study also has several limitations. The temporal and spatial scope is limited to specific coastal regions of Central Java, which may not fully capture the variability in other regions or inland areas. However, the study focuses primarily on ENSO and IOD as climate drivers, while other influential factors such as the Madden–Julian Oscillation (MJO), monsoonal patterns, or regional topography were not explicitly considered. For future research, it is recommended to expand the spatial coverage to include inland and upland areas, and to integrate additional atmospheric–oceanic indices such as MJO or the Pacific Decadal Oscillation (PDO) for a more comprehensive analysis. Utilizing higher-resolution spatial data and applying advanced statistical or machine learning

techniques may improve the understanding of complex relationships among multiple variables.

References

- Abdullah, S. E. A. N. A. (2021). Analisis hubungan indeks Niño 3.4 dengan curah hujan di Jawa Tengah. *Buletin Meteorologi, Klimatologi dan Geofisika*, 2(1), 24-30.
- Afghani, F. A., Mashuri, I., Khirtin, R., & Cahyo, M. A. (2023). Topography Effects on Rainfall Characteristics in Bandung City and Cilacap Regency for the 2016-2020 Period. *Sainmatika: Jurnal Ilmiah Matematika dan Ilmu Pengetahuan Alam*, 20(2), 157-167.
- Agustina, L., Syawreta, A., & Irawan, A. M. (2020). Analisis Ambang Batas Hujan untuk Pengembangan Sistem Peringatan Dini Tanah Longsor: Studi Kasus Kecamatan Pejawaran, Kabupaten Banjarnegara, Provinsi Jawa Tengah. *Jurnal Dialog Penanggulangan Bencana*, 11(1), 75-81.
- Alavinia, S. H., & Zarei, M. (2021). Analysis of spatial changes of extreme precipitation and temperature in Iran over a 50-year period. *International Journal of Climatology*, 41(S1), E2269-E2289.
- Aldrian, E., & Djamil, Y. S. (2008). Spatio-temporal climatic change of rainfall in East Java Indonesia. *International Journal of Climatology*, 28(4), 435-448.
- Amri, S., & Giarno, G. (2024). Analisis Dinamika Atmosfer Pada Kejadian Banjir, Tanah Longsor, dan Angin Kencang Di Semarang dan Demak Tanggal 13 Maret 2024. *Jurnal Ilmiah Biosaintropis (Bioscience-Tropic)*, 10(1), 77-89.
- Anam, A. R., Asfahanif, F., Muthi'ah, V. D., Pangedoan, A. D., & Giarno, G. (2023). Comparison Analysis of Wind Patterns and Its Correlations to Temperature, Humidity, and Rainfall in Coastal and Non-Coastal Areas. *EKSAKTA: Berkala Ilmiah Bidang MIPA*, 24(01), 67-79.
- Ashok, K., Guan, Z., & Yamagata, T. (2001). Impact of the Indian Ocean dipole on the relationship between the Indian monsoon rainfall and ENSO. *Geophysical research letters*, 28(23), 4499-4502.
- Ashok, K., & Saji, N. (2007). On the impacts of ENSO and Indian Ocean dipole events on sub-regional Indian summer monsoon rainfall. *Natural Hazards*, 42, 273-285.
- Biswas, J. (2023). Unravelling the influence of teleconnection patterns on monsoon extreme precipitation indices over the Sikkim Himalayas and West Bengal. *Journal of hydrology*, 618, 129148.
- Cai, W., Santoso, A., Wang, G., Weller, E., Wu, L., Ashok, K., . . . Yamagata, T. (2014). Increased frequency of extreme Indian Ocean Dipole events due to greenhouse warming. *Nature*, 510(7504), 254-258.
- Chakraborty, A., & Singhai, P. (2021). Asymmetric response of the Indian summer monsoon to positive and negative phases of major tropical climate patterns. *Scientific Reports*, 11(1), 22561.
- Darmawan, Y., Mashuri, I., Jumansa, M. A., Aslam, F. M., & Azzahra, A. (2023). Analisis Daerah Rawan Banjir dengan Metode Composite Mapping Analysis (CMA) di Kota Padang. *Jurnal Ilmiah Geomatika*, 29(2), 89-97.
- Donat, M., Alexander, L. V., Yang, H., Durre, I., Vose, R., Dunn, R. J., . . . Caesar, J. (2013). Updated analyses of temperature and precipitation extreme indices since the beginning of the twentieth century: The HadEX2 dataset. *Journal of Geophysical Research: Atmospheres*, 118(5), 2098-2118.

- Fadlan, A., Sugianto, D. N., Kunarso, K., & Zainuri, M. (2017). Pengaruh fenomena monsun, El Niño southern oscillation (Enso) dan Indian Ocean Dipole (IOD) terhadap anomali tinggi muka laut di utara dan selatan Pulau Jawa.
- Giarno, G., & Nanaruslana, Z. (2022). The precursors of high rainfall intensity during June in Southern Central Java: A case study of flash floods 18 june 2016 in Purworejo. *MAUSAM*, 73(4), 867-886.
- Goddard, L., & Gershunov, A. (2020). Impact of El Niño on weather and climate extremes. *El Niño Southern Oscillation in a changing climate*, 361-375.
- Hendon, H. H. (2003). Indonesian rainfall variability: Impacts of ENSO and local air-sea interaction. *Journal of Climate*, 16(11), 1775-1790.
- Hidayat, N. M., Pandiangan, A. E., & Pratiwi, A. (2018). Identifikasi perubahan curah hujan dan suhu udara menggunakan Rclimindex Di wilayah Serang. *Jurnal Meteorologi Klimatologi dan Geofisika*, 5(2), 37-44.
- Hidayat, R., Ando, K., Masumoto, Y., & Luo, J. (2016). *Interannual variability of rainfall over Indonesia: Impacts of ENSO and IOD and their predictability*. Paper presented at the IOP Conference Series: Earth and Environmental Science.
- Ikhwal, M., Nur, S., Darmansyah, D., Hamdan, A., Ersan, N., Aida, N., . . . Satria, A. (2022). *A review of climate change studies on paddy agriculture in Indonesia*. Paper presented at the IOP Conference Series: Earth and Environmental Science.
- JMA. (2002). Indian Ocean Dipole (IOD) / Historical IOD Events.
- Kunarso, K., Hadi, S., Ningsih, N. S., & Baskoro, M. S. (2011). Variabilitas suhu dan klorofil-a di daerah upwelling pada variasi kejadian ENSO dan IOD di perairan selatan Jawa sampai Timor. *ILMU KELAUTAN: Indonesian Journal of Marine Sciences*, 16(3), 171-180.
- Kurniadi, A., Weller, E., Min, S.-K., & Seong, M.-G. (2021). Independent ENSO and IOD impacts on rainfall extremes over Indonesia. *International Journal of Climatology*, 41(6), 3640-3656.
- Lee, H., Calvin, K., Dasgupta, D., Krinner, G., Mukherji, A., Thorne, P., . . . Barrett, K. (2023). Climate change 2023: synthesis report. Contribution of working groups I, II and III to the sixth assessment report of the intergovernmental panel on climate change.
- Mardiansyah, W., Setiabudidaya, D., Khakim, M. Y. N., Yustian, I., Dahlan, Z., & Iskandar, I. (2018). On the influence of Enso and IOD on rainfall variability over the Musi Basin, South Sumatra. *Science and Technology Indonesia*, 3(4), 157-163.
- McBride, J. (1998). Indonesia, Papua New Guinea, and tropical Australia: the southern hemisphere monsoon. *Meteorology of the Southern Hemisphere* (pp. 89-99): Springer.
- McBride, J. L., & Nicholls, N. (1983). Seasonal relationships between Australian rainfall and the Southern Oscillation. *Monthly weather review*, 111(10), 1998-2004.
- Nabila, N. M., Sasmito, B., & Sukmono, A. (2019). Studi karakteristik gelombang perairan Laut Jawa menggunakan satelit altimetri tahun 2016-2018 (studi kasus: perairan laut Utara Jawa). *Jurnal Geodesi Undip*, 9(1), 67-76.
- Nandargi, S., & Barman, K. (2018). Evaluation of climate change impact on rainfall variation in West Bengal. *Acta Sci. Agric*, 2(7).
- NOAA. (2025). Cold & Warm Episodes by Season.

- Raharja, A. B., Faqih, A., & Setiawan, A. M. (2022). An Application of Deep Learning Technique to Improve Subseasonal to Seasonal Rainfall Forecast over Java Island, Indonesia. *Jurnal Pengelolaan Sumberdaya Alam dan Lingkungan (Journal of Natural Resources and Environmental Management)*, 12(4), 587-598.
- Rahayu, H. P., Haigh, R., Amaratunga, D., Kombaitan, B., Khoirunnisa, D., & Pradana, V. (2020). A micro scale study of climate change adaptation and disaster risk reduction in coastal urban strategic planning for the Jakarta. *International Journal of Disaster Resilience in the Built Environment*, 11(1), 119-133.
- Rahayu, N. D., Sasmito, B., & Bashit, N. (2018). Analisis pengaruh fenomena Indian Ocean Dipole (IOD) terhadap curah hujan di pulau Jawa. *Jurnal Geodesi Undip*, 7(1), 57-67.
- Rahman, M. S., Toiba, H., & Huang, W.-C. (2021). The impact of climate change adaptation strategies on income and food security: Empirical evidence from small-scale fishers in Indonesia. *Sustainability*, 13(14), 7905.
- Saji, N., Goswami, B. N., Vinayachandran, P., & Yamagata, T. (1999). A dipole mode in the tropical Indian Ocean. *Nature*, 401(6751), 360-363.
- Setyawan, W. B., & Pamungkas, A. (2017). *Perbandingan karakteristik oseanografi pesisir utara dan selatan Pulau Jawa: pasang-surut, arus, dan gelombang*. Paper presented at the Prosiding Seminar Nasional Kelautan dan Perikanan III.
- Supari, Tangang, F., Salimun, E., Aldrian, E., Sopaheluwakan, A., & Juneng, L. (2018). ENSO modulation of seasonal rainfall and extremes in Indonesia. *Climate Dynamics*, 51, 2559-2580.
- Suwarman, R., Riawan, E., Simanjuntak, Y. S. M., & Irawan, D. E. (2022). Kajian perubahan iklim di pesisir Jakarta berdasarkan data curah hujan dan temperatur. *Buletin Oseanografi Marina*, 11(1), 99-110.
- Trenberth, K. E. (1997). The definition of el Niño. *Bulletin of the American Meteorological Society*, 78(12), 2771-2778.
- Veanti, D. P. O., & Kloster, S. (2018). *The change in forest fire danger and burnt area related to the change in meteorological forcing variability*. Paper presented at the AIP Conference Proceedings.
- Xiao, C., Ye, J., Esteves, R. M., & Rong, C. (2016). Using Spearman's correlation coefficients for exploratory data analysis on big dataset. *Concurrency and Computation: Practice and Experience*, 28(14), 3866-3878.
- Yulihastin, E., Muhammad, F., & Sofiaty, I. (2021). Oceanic effect on precipitation development in the maritime continent during anomalously-wet dry seasons in Java. *The Indonesian Journal of Geography*, 53(3), 328-339.
- Yunus, R. (2015). *Efek Fenomena Iklim Global Dan Topografi Terhadap Pola Distribusi Curah Hujan Di Provinsi Jawa Tengah Dan Di Yogyakarta*. Universitas Gadjah Mada.
- Zar, J. H. (2005). Spearman rank correlation. *Encyclopedia of biostatistics*, 7.